MAGNETIC CLEANLINESS ACTIVITIES IN ADVANCED NANOSATELLITES SYSTEMS FOR EARTH OBSERVATION RESEARCH - ANSER MISSION

Sergio. F. Romero [(1)], M.A. Rivero Rodriguez [(2)], Marina Díaz Michelena [(1)], Álvaro Román de Aragón [(2)] and Santiago Rodríguez Bustabad [(3)]

[(1)] Space Magnetism Area of the Payloads and Space Sciences Department, INTA, Madrid, Spain, Email: fdezrs@inta.es
[(2)] ISDEFE as External Consultant for INTA, Madrid, Spain, Email: riverorma.pers_externo@inta.es
[(3)] Space Programs Department, INTA, Madrid, Spain, Email: rodriguezs@inta.es

ABSTRACT

The purpose of this paper is to describe the specific magnetic measurements that must be made on the flight model ANSER (Advanced Nanosatellites Systems for Earth observation Research) satellite to ensure the necessary magnetic cleanliness, to characterize the magnetic torques, and to verify the magnetometer measurements. The objective is to develop the necessary technology to implement future space missions based on Satellite Constellations. This article describes both the innovative measurement procedures used and the measurement uncertainty calculations. The results obtained from both Cube Sats and the most important magnetic elements are presented, including the determination of the remaining and induced magnetic moment of spacecraft, and the calibration or characterization of magnetometers and magnetic torquers.

1. INTRODUCTION

ANSER (Advanced Nanosatellites Systems for Earth observation Research) is the first Earth observation mission developed and funded by INTA's Small Satellite Constellations programme. The objective is to develop the necessary technology to implement future space missions based on Satellite Constellations. The ANSER mission has been designed to study and monitor the quality of continental waters (reservoirs and wetlands located on the Iberian Peninsula) using space remote sensing techniques (see Fig. 1). It is a pilot mission and will lay the foundations for the development of the key technology for the implementation of distributed missions on Nanosatellite Constellations [1]. One of the main objectives of the project is to improve the pointing accuracy of the payload during the formation flights of these satellite constellations. To achieve this objective, the magnetic characterization of the platform, as well as the performance of its magnetic equipment, has been considered very critical.

Although much progress has been made in the verification of miniaturized equipment for use in Cube Sats, there are few published studies on magnetic cleanliness measures or on the characterization of the magnetic devices they use. References [2] and [3] are articles that theoretically deal with magnetic cleanliness strategy in this type of satellites. References [4-6] deal with the tests and simulations that can be done on the ground to check the operation of the attitude determination and control system (ADCS). In [4] and [5] measurements are made on a testbed and the magnetic fields generated by a Helmholtz cage for the experimental verification of magnetic based attitude control techniques for nanosatellites. In [6] the de-tumbling control of a CubeSat is evaluated by simulations.

The ANSER mission objectives are detailed in section 2. The approximate dimensions of the satellites are 30x10x10 cm^3 in non-deployed configuration, and, with the panels deployed, the upper area increases to 70x30 cm^2 (see Fig. 1). Its approximate weight is 3.4 kg.

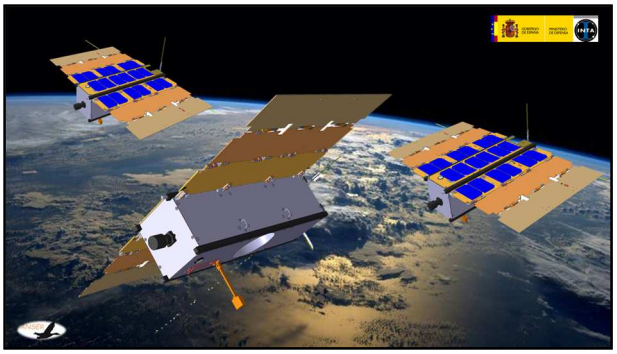

Figure 1. ANSER satellite constellation

Section 3 describes the facility and the test methods used during the magnetic characterization of the ANSER satellites. The ANSER (ADCS) includes magnetometers, 3 reaction wheels, as well as 3 magnetic torquers, a start tracker, a high precision solar sensor (CMOS camera), one horizon sensor (CMOS camera), 3 rate sensors (MEMS) and 10 low resolution solar sensors (photodiodes). Section 4 details the results for the determination of the residual and induced magnetic moment of complete satellites, and the characterization of on-board magnetometers and magnetic torquers. Also, a discussion and a measurement uncertainty study have been carried out on the results obtained. Finally, the conclusions of the study are explained in section 5.

2. ANSER SATELLITE CONSTELLATION DESCRIPTION

The objective of ANSER is to develop and demonstrate enabling technologies for future and efficient Earth Observation (EO) missions, making use of four main novel concepts: constellations of nanosatellites, formation flying, fractionated instruments, and miniaturized optical technologies.

Throughout the last decades, and from the first meteorological mission TIROS-1 in 1960, hundreds of EO satellites and missions have been launched to provide critical and useful information in many disciplines of Earth science, such as meteorology, vegetation, atmosphere, biology, oceanography, or disaster surveillance. According to the growth and evolution of space technology, size, mass, and capability of EO satellites have been gradually increasing from a few tens of kilograms to several tons. Technology allowed for including in the same platform several instruments operating synergistically to efficiently produce better and more accurate data. It was assumed that, because that instrumentation shared platform resources, such as power, buses, communications, launch, etc., the overall mission costs should be lower.

Nevertheless, reality proved that the high inherent complexity of such solutions, combined with a limited compatibility between instruments operation, plus many programmatic added difficulties and significant scheduling delays, shot up the final mission costs.

For this reason, other technical approaches to EO missions are being explored and promoted by government and international institutions, while new solutions in line with the NewSpace concept -which is being leaded today by very competitive small companies focused on small and very small space platforms (nanosatellites and microsatellites)- should be taken into account.

In the last years, systems based on nanosatellites (small satellites under 10 kg of mass) became an attractive solution for new scientific and technological space missions. In particular, CubeSats turned from being a fast and cheap way to access space for Universities, into a highly-valued spacecraft standard for many commercial and government sectors, because of their shorter development times, lower costs (including launch cost), fast access to new components or miniaturized sensors, and improved functionality.

Nevertheless, operative Earth observation missions keep being a challenge for such very small satellites because of their limitations in terms of available power, capability to combine high ground coverage with high spatial resolution, short revisit times, etc. In addition to that, the risks of using commercial off-the-shelf (COTS) components and non-space qualified units should be assessed when an operative nanosatellite mission is being planned. For these reasons, distributed systems, satellite constellations, and miniaturization concepts must be taken into account when working with small satellites to have real chances of achieving operational Earth observation missions.

The strategic objective of ANSER, to develop a set of key enabling technologies to make INTA into a relevant actor for planning, developing, and exploitation low cost and high performance Earth Observation missions, is broken down into four specific objectives:

• Objective 1: To develop an efficient and stable formation flying control system for nanosatellites compatible with Earth observation requirements.

• Objective 2: To develop a highly-accurate Attitude Determination and Control System (ADCS) for nanosatellites which enables coordinated pointing of the fractionated instrument constrained by the formation flying and which paves the way to reach 60 m of spatial resolution on ground.

• Objective 3: To develop a multi-node Inter-Satellite Link (ISL) equipment for nanosatellites control and coordination.

• Objective 4: To develop a miniaturized optical payload for Earth observation (CINCLUS) to work as a pilot mission for ANSER.

3. MAGNETIC CHARACTERIZATION AND TEST DESCRIPTION

3.1. Facility description

These measurements will be carried out at the INTA Space Magnetism Area singular facility K11. The facility has been constructed in an area of minimum magnetic field gradient. The building, isolated from other constructions, has a plant of 10 x 8 m^2, and has been built with non-magnetic materials (see Fig. 2.A). Temperature and humidity control is achieved by a system allocated 25 m away from the building and remotely controlled from the building. It is provided with two systems of three axes coils for a test volume in the order of 1 m side cube as well as a pair of coils for demagnetization. The coils systems are aligned with the magnetic North. The inner coils are used for the application of magnetic fields and outer coils (see Fig. 2.B), for the compensation of the geomagnetic field. The interior has been kept clear in order to allocate the voluminous electrical ground support equipment for the systems under test. Since commissioning, the magnetic cleanliness measurements of various space missions with demanding requirements such as Juice or Solar Orbiter [7, 8] have been performed at this facility.

Figure 2. A) INTA Facility; B) three axis Helmholtz coils used during the tests.

3.2. Methods and procedures

The method followed to calculate the residual magnetic dipole of the satellite in different modes of operation is based on [9] with some improvements. The measurement of the satellite is carried out in 4 stages: initial measurement (INITIAL) without cables, demagnetized (DEPERM) applying an AC signal of 3 Hz with 5000 µT amplitude successively on each XYZ axis, magnetized (PERM) applying a perm field of 300 µT on each XYZ axis and in the different operating modes (STRAY FIELD). For each calculation of the magnetic moment we use 7 fluxgate type magnetic sensors located on the East-West axis of the terrestrial magnetic field at different distances and pointing to the geometric centre of the satellite (see Fig 3). With this arrangement, it is possible to check the goodness of the fit of the field measurement to the calculation of the equivalent dipole moment, which should be proportional to r^{-3}. Finally, this measurement must be repeated for the 6 semi-axes of the satellite, turning the equipment on the turntable.

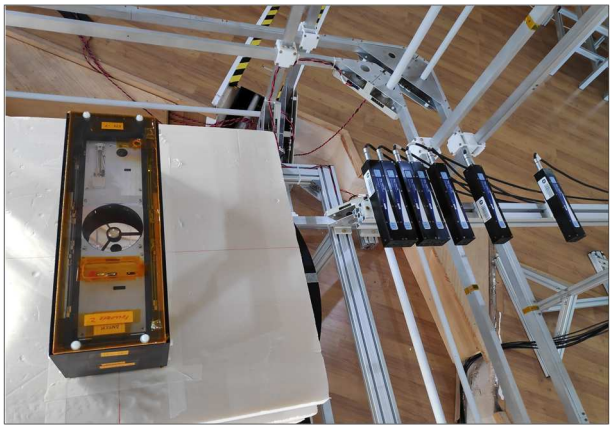

Figure 3. ANSER Follower and the 7 fluxgate magnetometers used during the tests.

For the measurement of the induced magnetic moment, the same arrangement of sensors was used and the following procedure was carried out. The Earth's magnetic field was compensated for by the external Helmholtz coil set. A measurement of the magnetic environment was made by applying external magnetic fields (-70 µT and +70 µT) on three axis. Afterwards, we repeat the measurement with the satellite on the turntable, applying (-70 µT and +70 µT) on each axis. Finally, we calculate the coefficient which provides the relationship between induced magnetic moment and the external field applied can be calculated as:

$$A_i = {}^{\Delta M_i}/_{\Delta B_i} \quad (1)$$

Where ΔM_i is the increment of the magnetic moment in the each axis calculated from the difference of the magnetic fields measured with and without satellite and ΔB_i is the increment of the magnetic field applied (140 µT in this case).

For the characterization of the on-board magnetometer, the following procedure was performed. The Earth's magnetic field was compensated by the external Helmholtz coil set. A magnetic field calibration was performed at the center of the table by applying external magnetic fields (from -50 µT to +50 µT in 5 µT steps) on each semi-axis using the internal Helmholtz coil set. Finally, the measurements were repeated with the on-board magnetometer of the satellite. Fig. 4 shows a picture of the measurement setup.

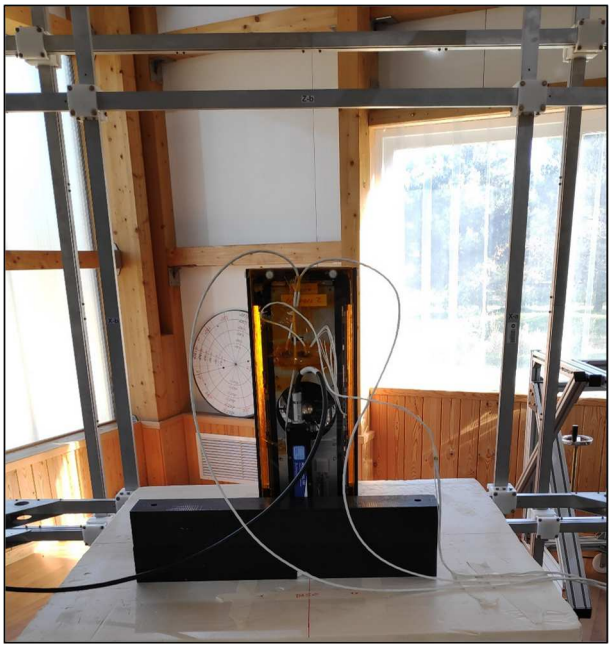

Figure 4. ANSER on-board magnetometer characterization measurement setup.

4. RESULTS AND DISCUSSION

4.1. Magnetic moment

The magnetic moment values of the different measurements obtained by dipole approximation of the field, with their uncertainty of the magnetic moment values are shown in the Tab. 1 for ANSER Leader satellite and in the Tab. 2 for ANSER Follower satellite.

Table 1. ANSER Leader magnetic moment values.

	m_x (mA·m²)	m_y (mA·m²)	m_z (mA·m²)	|m| (mA·m²)
Initial	-140.3 ± 3	-4.7 ± 1	-23.4 ± 2	142.3 ± 3
After DEPERM	1.7 ± 1	-1.3 ± 1	-3.5 ± 1	4.2 ± 2
After PERM	3.6 ± 2	1.2 ± 1	-1.9 ± 1	4.3 ± 3
EPS+OBC Mode	1.7 ± 1	-1.7 ± 3	-3.8 ± 1	4.5 ± 3
Detumbling+ Mode	-337.5 ± 6	-336.0 ±6	333.3 ± 6	581.3 ±11
Navigation Mode	0.3 ± 1	-1.6 ± 3	-4.7 ± 1	4.9 ± 3
Observation Mode	1.3 ± 1	-1.5 ± 2	-4.9 ± 1	5.3 ± 3

Table 2. ANSER Follower magnetic moment values.

	m_x (mA·m²)	m_y (mA·m²)	m_z (mA·m²)	|m| (mA·m²)
Initial	-13.3 ± 1	-69.7 ± 2	-36.3 ± 2	79.7 ± 3
After DEPERM	-14.1 ± 1	-6.2 ± 1	-8.2 ± 1	17.4 ± 2
After PERM	-12.0 ± 1	-6.9 ± 1	-4.0 ± 1	14.4 ± 2
EPS+OBC Mode	-11.0 ± 1	-3.7 ± 2	-5.7 ± 1	12.9 ± 2
Detumbling+ Mode	-348.9 ± 6	-340.7 ± 6	335.4 ± 6	591.4 ± 11
Navigation Mode	-12.1 ± 1	-4.5 ± 1	-8.8 ± 1	15.6 ± 2
Observation Mode	-11.6 ± 1	-5.1 ± 2	-9.2 ± 2	15.7 ± 2

Taking into account the results of the previous tables, the ANSER project satellites studied have a very low remaining magnetic moment after demagnetization. The differences found between the two satellites must be due to the payloads they carry on board. The value of the magnetic moment in the detumbling mode is only informative since during this functional mode the CubeSat magnetic torques are trying to correct their attitude generating a larger magnetic dipole moment. To check its operation, a measurement was made with an acquisition frequency of 1 kHz at the maximum duty cycle that is allowed 80% (see Fig. 5). In the Fig. 5 you can see, in blue, the magnetic field measurement for the positive Z semi-axis (Bz+) with and without the satellite in operation; and, in red, the same for the negative Z semi- axis (Bz-).

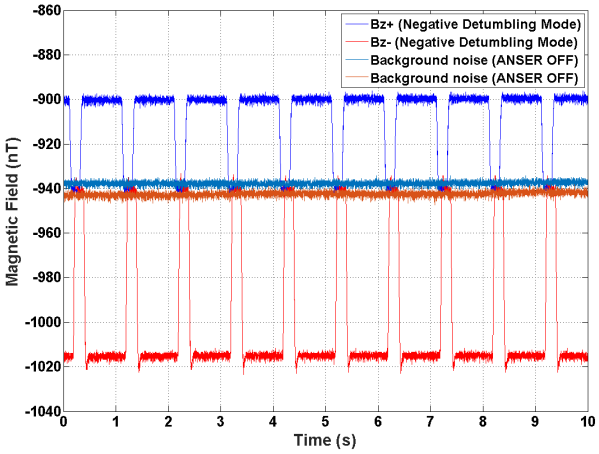

Figure 5. ANSER magnetic torquer characterization

4.2. Induced magnetic moment

The induced magnetic moment calculated according Eq. 1 are shown in Tab. 3.

Table 3. Ratio of the magnetic moment components and the applied field.

	A_x (mA·m²/μT)	A_y (mA·m²/μT)	A_z (mA·m²/μT)
Leader	0.39 ± 0.01	0.44 ± 0.01	0.46 ± 0.01
Follower 2	0.37 ± 0.01	0.41 ± 0.01	0.42 ± 0.01

In this case the magnetic behavior of the two satellites is very similar. These values of induced magnetic moment could be considered small. However, in this case, we must consider them moderate because they can generate magnetic moments of the order of 20 mA·m² in the worst case, which are of the same order as the remaining magnetic moment of the satellites.

4.3. Magnetometer characterization

The characterization of the on-board magnetometer using the raw data obtained from ADCS software is presented in the Figs 5, 6 and 7.

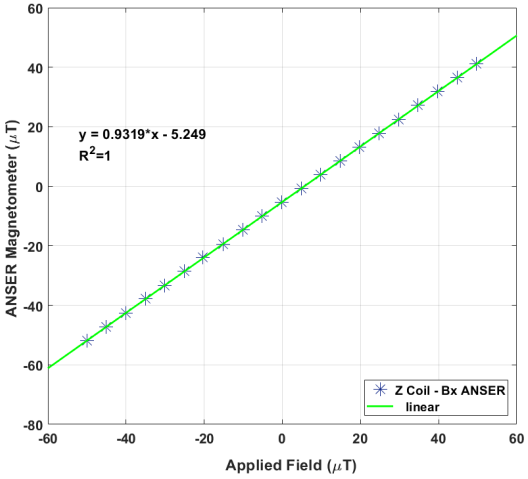

Figure 6. ANSER characterization of the on-board magnetometer X- Axis.

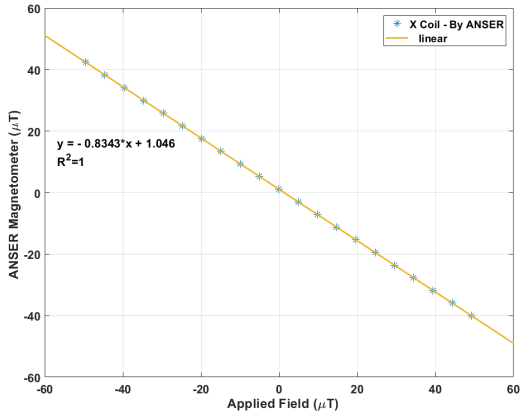

Figure 7. ANSER characterization of the on-board magnetometer Y- Axis.

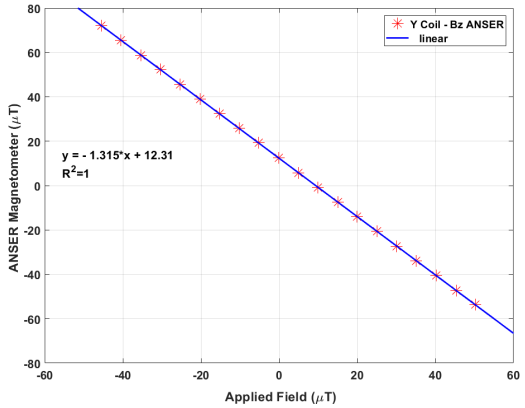

Figure 8. ANSER characterization of the on-board magnetometer Z- Axis.

As can be seen in the previous graphs, the data from the on-board magnetometer show linear behavior within the expected operating margin. Therefore, a correct measurement value is to be expected when performing the in-orbit calibration routine.

4.4. Measurement uncertainty study

As mentioned above, we use several aligned sensors to measure the field at different distances simultaneously. Then, we perform a linear regression of its proportionality with r^3 and the goodness of fit of these data offers an evaluation of the quality of the calculation by the equivalent dipole moment method. The measurement uncertainty has been calculated according to [10] using the statistical analysis of a linear regression:

$$B = a + mx \;\; with \; x = \frac{\mu_0}{4\pi}\frac{2}{r^3} \tag{2}$$

where B is magnetic field in Teslas, m is magnetic moment in $A \cdot m^2$ and r is distance in meters. Then m and a can be calculated from the data as:

$$m = \frac{\sum_{i=1}^{N} x_i B_i - (\sum_{i=1}^{N} x_i)(\sum_{i=1}^{N} B_i)}{N\sum_{i=1}^{N} x_i^2 - (\sum_{i=1}^{N} x_i)^2} \tag{3}$$

$$a = \frac{\sum_{i=1}^{N} B_i - m\sum_{i=1}^{N} x_i}{N} \tag{4}$$

where N is the number of data. And, finally, the uncertainty of Δm and Δa can be calculated with the following expressions:

$$\Delta m = \frac{\sqrt{N}\,\sigma}{\sqrt{N\sum_{i=1}^{N} x_i^2 - (\sum_{i=1}^{N} x_i)^2}} \tag{5}$$

$$\Delta a = \Delta m \sqrt{\frac{\sum_{i=1}^{N} x_i^2}{N}} \tag{6}$$

where σ is defined as:

$$\sigma = \sqrt{\frac{\sum_{i=1}^{N} (B_i - a x_i - m)^2}{N-2}} \tag{7}$$

The measurement uncertainties presented in Tab. 1, 2 and 3 are calculated with this method. In Fig. 9 we can see an example of application on a linear regression of the experimental data. In future works, the authors will study other sources of uncertainty, such as deviations in distance or temperature, to improve the calculation of the total uncertainty.

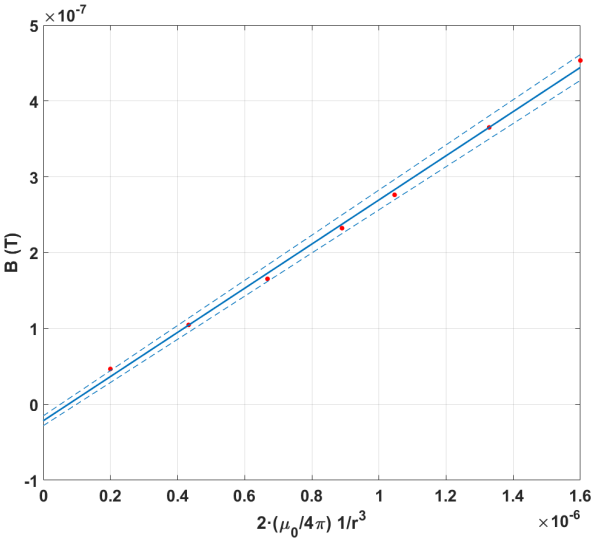

Figure 9. Example of measurement uncertainty calculation using a linear regression.

5. CONCLUSIONS

In this article the results of the magnetic measurements of two CubeSat satellites of the ANSER project for earth observation have been presented. The results stand out for being two units with a very low level of magnetic moment, both remanent and induced. Likewise, the verification of the magnetic devices on board has been carried out and it is also satisfactory.

In addition, a method for calculating the magnetic moment has been presented that substantially improves the procedure recommended in current regulations. Likewise, the calculation of the measurement uncertainties of this new method has been described.

As future work, the authors want to implement improvements in the ADCS of the satellites that form the constellation to achieve objective 2 of the ANSER project: to develop a high-precision ADCS for nanosatellites that allows the coordinated pointing of the fractional instrument constrained by the formation flying and which paves the way to reach 60m spatial resolution on the ground.

6. ACKNOWLEDGMENT

The authors wish to thank all the ANSER Project staff for their support in carrying out these measurements. This work has been funded by the Spanish Programme for Research, Development and Innovation under the reference PID2020-119208RB-I00 (MINOTAUR).

7. REFERENCES

1. N.H. Crisp, K. Smith and P. Hollingsworth, “Launch and deployment of distributed small satellite systems,” Acta Astronautica., vol. 114, pp. 65-78, October. 2015.

2. A. Lassakeur and C. Underwood, "Magnetic Cleanliness Program on CubeSats for Improved Attitude Stability," 2019 9th International Conference on Recent Advances in Space Technologies (RAST), 2019, pp. 123-129, doi: 10.1109/RAST.2019.8767816

3. A. S. K. Habila and W. H. Steyn, "In-orbit Estimation of the Slow Varying Residual Magnetic Moment and Magnetic Moment Induced by the Solar Cells on CubeSat Satellites," 2020 International Conference on Computer, Control, Electrical, and Electronics Engineering (ICCCEEE), 2021, pp. 1-6, doi: 10.1109/ICCCEEE49695.2021.9429618

4. A. Bahu and D. Modenini, "On-ground experimental verification of magnetic attitude control for nanosatellites," 2021 IEEE 8th International Workshop on Metrology for AeroSpace (MetroAeroSpace), 2021, pp. 568-573, doi: 10.1109/MetroAeroSpace51421.2021.9511720

5. G. Cervettini, S. Pastorelli, H. Park, D. Y. Lee and M. Romano, "Development and Experimentation of a CubeSat Magnetic Attitude Control System Testbed," in IEEE Transactions on Aerospace and Electronic Systems, vol. 57, no. 2, pp. 1345-1350, April 2021, doi: 10.1109/TAES.2020.3040032

6. W. Lu, L. Duan and Y. Cai, "De-tumbling Control of a CubeSat," 2018 IEEE International Conference on Advanced Manufacturing (ICAM), 2018, pp. 298-301, doi: 10.1109/AMCON.2018.8614819

7. M. D. Michelena, A. A. O. Cencerrado, J. de Frutos Hernansanz and M. Á. R. Rodríguez, (2019) "New Techniques of Magnetic Cleanliness for Present and Near Future Missions," 2019 International Symposium on Electromagnetic Compatibility - EMC EUROPE, pp. 727-730, doi: 10.1109/EMCEurope.2019.8872024

8. ESA/SRE(2014)1 ”JUICE JUpiter ICy moons Explorer Exploring the emergence of habitable worlds around gas giants” European Space Agency, September 2014.

9. ECSS-E-ST-20-07C Rev. 1 – Space Engineering – Electromagnetic Compatibility. European Cooperation for Space Standardization (ECSS), ESA-ESTEC, 7th February 2012.

10. Mook, W.G., “Errores, Medias y Ajustes” Chapter 13 of Isotopos Ambientales en el Ciclo Hidrológico, IGME, ISBN: 84-7840-465-1, 2003